Journal of Electronic Materials (2022) 51:4248–4256
https://doi.org/10.1007/s11664-022-09598-4

ORIGINAL RESEARCH ARTICLE

Facile Lithiophilic 3D Copper Current Collector for Stable Li Metal Anode

Qiang Zhao[1,2] · Jiayan Li[1] · Xin Chen[1] · Yongqi Zhang[2,3]

Received: 25 January 2022 / Accepted: 21 March 2022 / Published online: 7 May 2022

Abstract

Lithiophilic hosts are confirmed to effectively enhance the electrochemical stability of lithium (Li) anodes, thereby guaranteeing the safe, practical application of Li metal as the anode in rechargeable Li-ion batteries. This study reveals a lithiophilic three-dimensional copper current collector (Ag@CF). Silver (Ag) nanoparticles were anchored on the surface of a skeleton of copper foam (CF) via a facile displacement reaction under ultrasonic conditions. The introduced Ag nanoparticle layer reduces the nucleation barrier of Li, leading to a homogeneous Li nucleation and plating. Simultaneously, porous Ag@CF provides the structural support and storage volume of the Li anode, eliminating its volume change in the process of plating/stripping. Benefiting from the above, the Ag@CF electrode shows a superior electrochemical performance in half-type cells (near 100% coulomb efficiency for 350 cycles at 1 mA cm^{-2}). Composite electrodes (Li-Ag@CF) preloaded in the Ag@CF network deliver an ultra-long lifespan of over 1600 h with a low over-potential at 1 mA cm^{-2} in Li-Ag@CF symmetric cells. Furthermore, $LiFePO_4$|Li-Ag@CF full cells display enhanced capacity retention (over 80% for 800 cycles at 1 or 3 C). More importantly, this method is facile, large-scalable, and low-cost, which offers an alternation strategy for the practical application of stable Li anodes.

Graphical Abstract

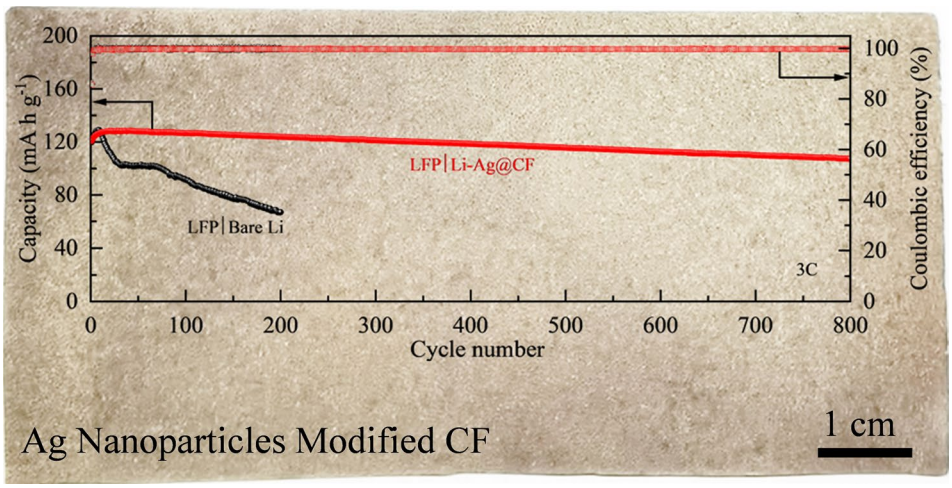

Keywords Li composite electrode · lithiophilic 3D copper current collector · ultra-long lifespan · enhanced capacity retention

✉ Yongqi Zhang
yqzhang@uestc.edu.cn

Extended author information available on the last page of the article

Introduction

With the promotion of distributed generation, such as solar and wind energy, and the continuous development of electrical products, energy storage devices with both high-energy density and high stability have been in the limelight.[1,2] Currently, lithium-ion batteries (LIBs) are the mainstream rechargeable energy storage devices, which have been widely assembled in portable electronic products and electric vehicles to provide electricity.[3–5] However, intrinsic properties (e.g., low specific capacity or instability) of the electrodes limit the further increase in the energy density of LIBs.[6] The lithium (Li) metal electrode (with the ultrahigh theoretical specific capacity and lowest electrochemical potential) is regarded as the key anode material to promote the revolution of rechargeable energy storage devices.[7,8] Unfortunately, pure Li metal is a hostless electrode, and usually tends to an uneven plating/stripping during the process of charging/discharging, even in the shape of a branch (dendrite growth).[9–11] The uneven plating/stripping of Li will lead to a series of problems, such as the formation of dead Li, the destruction of the solid electrolyte interphase (SEI) membrane and the consumption of limited Li resources, which give rise to a decrease in capacity and coulombic efficiency.[12–14] Under the worst case, the dendrite of Li may pierce the separator, resulting in serious safety incidents. In addition, due to the lack of support of the host materials, a pure Li anode will undergo a huge volume change during the process of charging/discharging. This will increase the instability of the LIBs, and even deteriorate their performance. All these inherent shortcomings hinder Li metal from directly acting as an anode of LIBs.

Many strategies have been carried out to address these issues. Electrolyte additives[15–20] and artificial protective membranes[21–23] have been reported to effectively improve the interfacial stability and electrochemical properties of Li anodes. However, these strategies are still unsatisfactory for the needs of practical applications, especially in the case of high current and high capacity. Due to the high Young's modulus, solid electrolytes have been used in the design of all-solid-state LIBs to suppress the Li dendrites. However, the insufficient Li^+ conductivity and unfavorable interface resistance remain the critical challenges.[24,25] Recently, another strategy has attracted much attention to regulate the plating of Li, that is to design three-dimensional (3D) current collectors. As the host of Li anodes, 3D current collectors with high specific surface area[26,27] have been reported to limit the local current density and restrict the rapid formation of Li dendrites to a certain extent.[28–30] Driven by this idea, various porous conductive current collectors have been designed to improve the stability of Li metal anodes, such as porous metals,[31–33] porous carbon frameworks,[34–38] and porous metal-organic frameworks.[39,40] Unfortunately, despite 3D current collectors having been proved to mitigate the growth of Li dendrites and the huge change of volume, the higher energy barrier (the nucleation over-potential) of Li atoms deposited on common materials (which were used to design the 3D current collectors, such as Cu,[41] Ni, C, or metal–organics) is still an obstacle to the uniform deposition of Li. The nucleation and plating behavior of Li atoms on heterogeneous substrates were discussed by Cui.[42] Their results showed that Li atoms nucleated or plated on a heterogeneous substrate with poor lithiophilic property need to overcome a relatively high energy barrier, which was the source of the inhomogeneous plating of Li and even the formation of Li dendrites. Therefore, it is particularly important to enhance the lithiophilic property of 3D current collectors.[43–51] Regrettably, most designs undergo complex chemical or physical processes, making it difficult to promote the actual application. In addition, as alternative designs with huge application prospects, it is necessary to have a low-cost preparation process and raw materials.

Here, we report a facile lithiophilic 3D copper current collector prepared by a simple and reliable displacement reaction. Due to economy and practicability, copper foam (CF) was chosen as the basic framework to provide the space for Li deposition. The microporous structure of CF guarantees the infiltration of the electrolyte, which provides abundant channels for the fast diffusion of the Li^+. Silver (Ag) nanoparticles were anchored on the surface of the skeleton of the CF via a displacement reaction under ultrasonic conditions. The operation of the displacement reaction under ultrasonic conditions is to remove those Ag nanoparticles with poor bonding on-site, and indemnify the remaining Ag nanoparticles which are firmly riveted on the surface of the CF. More importantly, Ag nanoparticles with certain Li solubility can reduce the nucleation over-potential of Li atoms, leading to a homogeneous deposition. Under the synergistic effect of the advantages mentioned above, the modified CF (Ag@CF) electrode and the modified Li composite electrode (Li-Ag@CF) can deliver an ultra-long lifespan in half-cells or symmetric cells, respectively. Furthermore, a full cell assembled with $LiFePO_4$ (LFP) and Li-Ag@CF was constructed to verify the practical application of this design, which displays enhanced cycling performances and over 80% capacity retention after 800 cycles at 1 and 3 C.

Experimental

Preparation of Ag@CF Electrode

All reagents were used without further purification. The CF (0.3 mm in thickness; Shenzhen Kejing Zhida Technology) was cleaned by anhydrous ethanol and deionized water to remove the impurities and oil stains on the surface. Then, the washed CF was immersed in 1 M hydrochloric acid for 20 min to remove the oxide layer. After that, the cleaned CF was washed with deionized water again and dried in a vacuum oven at 60°C for 2 h. To prepare the reaction solution, 0.25 ml of nitric acid and 42.5 mg of silver nitrate (both, Chengdu Kelong Chemical Reagent Factory) were added into 250 ml of deionized water and stirred for 15 min to obtain a clear liquid. Then, the CF was immersed in the reaction solution under ultrasonic conditions for 30 min. The frequency and power of the ultrasonics were 20 KHz and 0.05 W cm^{-2}, respectively. Finally, after cleaning with deionized water and drying in a vacuum oven at 60°C for 2 h, the Ag@CF electrode was obtained.

Preparation of Li-Ag@CF or Li-CF Electrodes and LFP Cathode

The composite electrodes/anodes (Li-CF and Li-Ag@CF) in symmetric cells and full cells were prepared by preloading 6 mA h cm^{-2} of Li in CF and Ag@CF and then harvesting from half-cells. All the electrodes disassembled from half-cells were cleaned several times using DMC in an Ar-filled glove box with O_2 and H_2O less than 0.01 ppm. Then, the pre-cleaned samples were dried at 60°C in a vacuum oven. To prepared the cathodes of the full cells, LFP, conductive carbon black (both, Shenzhen Kejing Zhida Technology Co), and polyvinylidene fluoride were mixed in the weight ratio of 8:1:1 and ground for 1 h. Then, the paste was uniformly applied to an aluminum foil and dried overnight at 80°C in a vacuum oven. Finally, the LFP cathodes were obtained by stamping the foils into a disc with the radius of 6 mm. The areal loading density of the active material per cell was about 2.3 mg cm^{-2}.

Electrochemical Performance

Electrochemical measurements were implemented using standard CR2032 button battery cells. All the cells were assembled in an Ar-filled glove box. A Celgard 2500 membrane was used as the separator. An mixture of 1 M Li bis-(trifluoromethane) sulfonylimine salt in 1:1 DOL/DME (volume ratio) with 1 wt% of $LiNO_3$ additive was used as the electrolyte, and the added amount of electrolyte was 50 ul per cell. CF, Ag@CF, and Li foil (450 μm in thickness) with a radius of 6 mm were used as the working electrodes and counter electrodes in the half-cells. Li-CF or Li-Ag@CF were assembled as the working electrodes in symmetric cells. Galvanostatic cycling was performed on a NEWARE battery test system. In order to enhance and stabilize the native SEI membrane, an initial 5 cycles with a low current density of 50 uA cm^{-2} were set. Impedance was measured using a CHI660e electrochemical workstation (Shanghai Chenhua Science Technology) from 0.01 Hz to 100 kHz. For full cells, LFP electrodes were used as cathodes, Li-Ag@CF electrodes or Li foils were used as anodes, and charge/discharge processes were implemented from 2.4 V to 3.8 V.

Characterization

Morphological characteristics and energy-dispersive spectroscopy (EDS) were estimated by scanning electron microscopy (SEM; FEI Verios 460). The structure and crystal phases of the samples were examined using x-ray diffraction (XRD; Rigaku Miniflex 600).

Results and Discussion

Figure 1a illustrates the design and strategy of the lithiophilic 3D copper current collector. Ag atoms were transferred from the solution to the surface of the skeleton of the

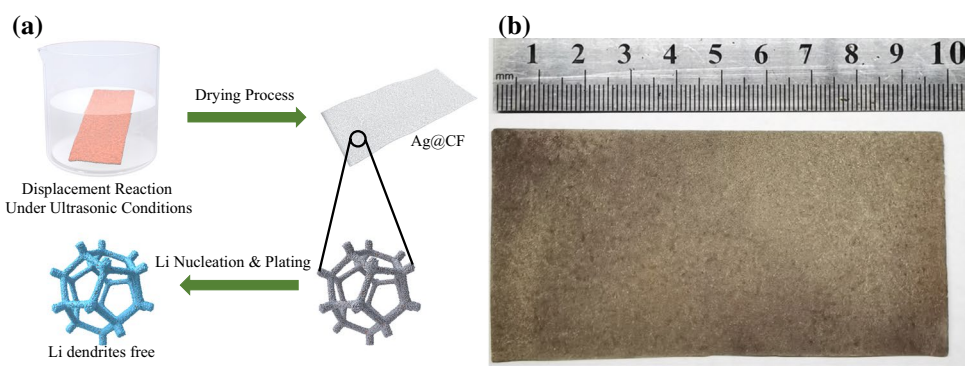

Fig. 1 (a) Scheme of the strategy for lithiophilic 3D Ag@CF; (b) digital image of Ag@CF of large scale.

CF via a displacement reaction to form an even Ag-modified layer. An Ag-modified layer has been reported to enhance the lithiophilicity of the hosts for Li anodes.[52] Unfortunately, poor binding between the Ag nanoparticles and the surface of the hosts leads to the deterioration of the electrochemical performance during long cycles.[43] In this strategy, the displacement reaction occurred under ultrasonic conditions, which guarantees that the Ag nanoparticles are anchored on the surface of the skeleton of the CF homogeneously and firmly. The benefit from the convenient preparation process is that this lithiophilic Ag@CF electrode can be manufactured on a large scale. Figure 1b shows a digital image of an Ag-CF electrode with a size of 10 cm. What is more, because of the base material (copper) being compatible with the current commercial anode current collector, and the production process being environmentally friendly, this strategy can be conveniently applied to LIBs.

XRD was conducted to analyze the crystal phase and purity of the products. As shown in Fig. 2a, all the characteristic peaks emerging in the curve can be assigned to Ag or Cu. There were no other diffraction peaks, which suggests that the Ag@CF was composed of high-purity Ag and Cu. With no other impurities being introduced by the displacement reaction, this also proves the reliability of this strategy. Surface SEM morphologies of Ag@CF with low (Fig. 2b) and high resolution (Fig. 2c) indicate that the skeleton of the CF was densely covered by Ag nanoparticles hundreds of nanometers in size. Ag nanoparticles have been proved to dissolve Li atoms to generate a solid solution layer on the surface of current collectors. Therefore, Li nucleation barriers can be effectively reduced due to the appearance of Ag, leading to a uniform nucleation and plating of Li.[42] The element distribution on the surface of the sample was identified by EDS. As shown in Fig. S1b, the Ag element was evenly distributed on the skeleton of the CF, with a content of about 32%. Figure 2d shows the fracture surface morphology of the Ag@CF. As expected, the Ag nanoparticles grew on the surface of the Cu framework in an embedded manner, which means that the Ag nanoparticles have a strong adhesion to the surface of the CF, which guarantees the stability of the electrode during long cycles. Meanwhile, different from the smooth surface of the original CF skeleton (Fig. S1a), the surface of the CF modified by the Ag nanoparticles was covered with "hills" and "gullies", which implies that there is an increased contact area between the electrolyte and the electrode. The increased contact area will limit the local current density and restrict the rapid growth of Li dendrites.[53,54]

In this strategy, Ag nanoparticles were introduced to make the nucleation of Li easier, so half-cells were assembled to verify the superior electrochemical behavior of the 3D current collectors. Figure 3a shows the voltage–capacity curves of CF and Ag@CF at 1 mA cm^{-2} in the first cycle. Different from the CF, the nucleation over-potential of Li on Ag@CF was significantly reduced, from 45 mV to 11

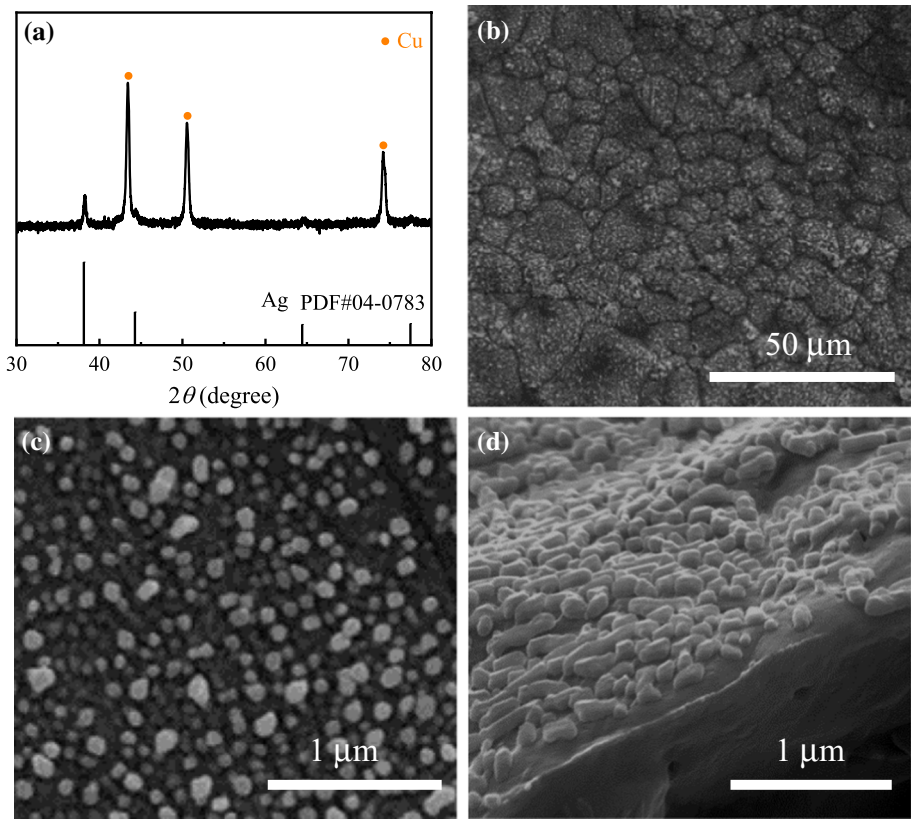

Fig. 2 (a) XRD curve of the Ag@CF. (b–d) SEM images of the Ag@CF.

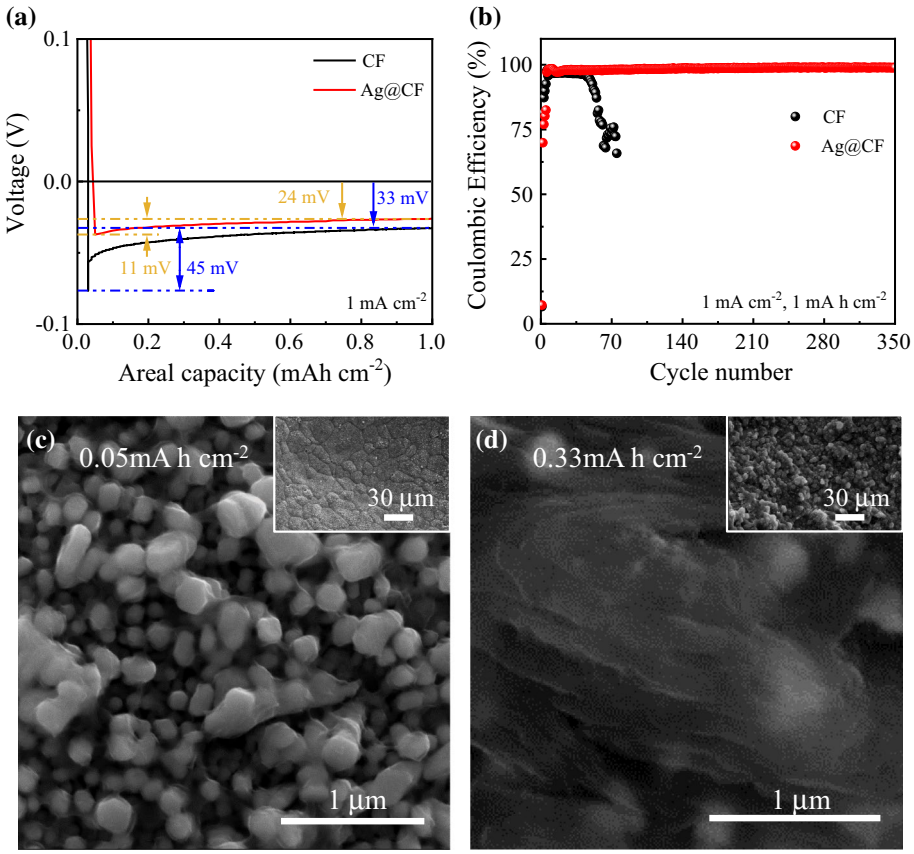

Fig. 3 (a) Voltage–capacity curves of Li plating on CF and Ag@CF in the first cycle. (b) Coulomb efficiency of CF and Ag@CF at 1 mA cm^{-2} with the area capacity of 1 mA h cm^{-2}. (c, d) Morphologies of Ag@CF with plating Li capacities of 0.05 and 0.33 mA h cm^{-2}.

mV. This reduction of the nucleation over-potential can be attributed to the Ag nanoparticles on the surface of the skeletons,[42,43,52] which will make the subsequent Li deposition uniform. The voltage–capacity curves at a lower current density (0.2 mA cm^{-2}) is revealed in Fig. S2. As shown, there is almost no energy barrier of Li atoms nucleating on the Ag@CF at 0.2 mA cm^{-2}, but an obvious nucleation over-potential still exists in the case of CF at 0.2 mA cm^{-2}. Furthermore, the electroplating voltage caused by the mass transfers resistance dropped from 33 to 24 mV. Superior nucleation over-potential and electroplating voltage means easier nucleation and plating of Li, which will suppress the formation of Li dendrites. As a key index to estimate the electrochemical stability of the modified 3D current collectors, coulombic efficiency (CE) was conducted in the half-cells. Figure 3b demonstrates the CE of Ag@CF at 1 mA cm^{-2} with a plating Li capacity of 1 mA h cm^{-2}. Obviously, the Ag@CF electrode delivers an enhanced CE compared with CF, which remained almost unchanged for 350 cycles. This implies that Ag@CF electrodes guarantee a more stable SEI membrane due to the more homogeneous deposition of Li.

In order to investigate the details of the initially deposition of Li on Ag@CF, the morphology evolution of Ag@CF electrodes was observed by SEM during the process of Li plating. Figure 3c and d reveals the micromorphologies of Ag@CF electrodes with plating capacities of 0.05 and 0.33 mA h cm^{-2}. (Insets show the morphologies with low resolution.) As expected, due to the favorable thermodynamics between Li and Ag, Li atoms prefer to deposit on the surface of Ag nanoparticles (Fig. 3c). This manner of deposition provides homogeneous nucleation sites for the subsequent deposition of Li.[42] Then, with the Li capacity increased to 0.33 mA h cm^{-2}, the surface of the Ag@CF was gradually covered by Li. Meanwhile, as can be seen in Fig. 3d, the Li deposition behavior was quite uniform, and there no Li dendrites can be observed. Different from the Ag@CF, the unmodified CF represented an undesirable Li deposition behavior (Fig. S3). Li atoms tend to deposit on the junction of the skeletons with the rapid growth of Li dendrites. This homogeneous nucleation and plating of Li on Ag@CF testifies that the modified 3D current collectors possess excellent lithiophilicity, thereby inhibiting Li dendrite growth, reducing dead Li generation, and enhancing the electrochemical stability.[47]

Symmetric cells (Li-Ag@CF|Li-Ag@CF) were constructed to evaluate the electrochemical stability of the composite electrodes using the 3D Ag@CF as host. Li-CF|Li-CF symmetric cells were also prepared as references. Figure 4a and b exhibit the voltage–time profiles of symmetric cells with cycling capacities of 1 mA h cm^{-2}and 3 mA cm^{-2} , respectively. As shown, the Li-Ag@CF electrodes achieved an ultra-long lifespan of more than 1600 h, with a mitigated

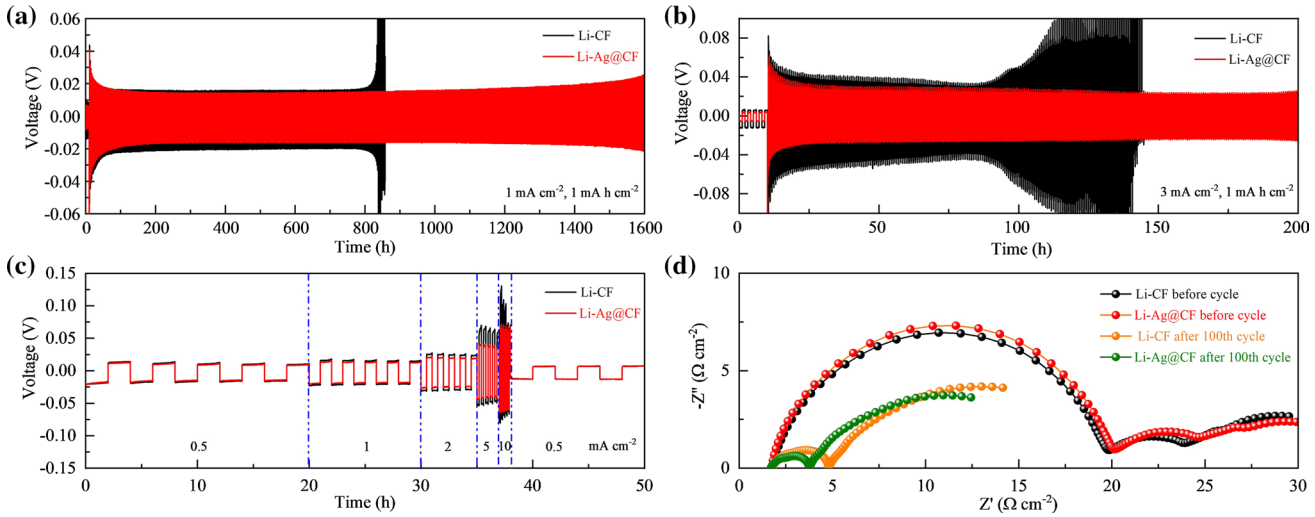

Fig. 4 Voltage–time profiles of Li-Ag@CF and Li-CF electrodes with cycling capacities of 1 mA h cm^{-2} at (a) 1 mA cm^{-2} and (b) 3 mA cm^{-2}. (c) Rate performance of the Li-Ag@CF and Li-CF electrodes. (d) Nyquist plots of Li-Ag@CF|Li-Ag@CF and Li-CF|Li-CF symmetric cells before and after 100 cycles of Li plating/striping.

voltage hysteresis of 30 mV at 1 mA cm^{-2}. In obvious contrast, the voltage hysteresis of the cells assembled by Li-CF electrodes sharply enlarged and fluctuated after 800 h, and were suddenly followed by a short circuit. In addition, at 3 mA cm^{-2} (Fig. 4b), and even at 5 mA cm^{-2} (Fig. S4), Li-Ag@CF electrodes still maintain a longer lifespan and lower voltage hysteresis, which indicates that the modified Ag@CF electrodes possess superior electrochemical stability. We believe that the superior electrochemical performance derives mainly from the modified surface of the CF. Ag nanoparticles anchored on the surface of the CF skeleton promote the electrochemical stability of Li-Ag@CF electrodes. To further verify the superiority of the modified composite electrodes, the morphology evolution of the composite electrodes after cycling was investigated by SEM. Fig. S5 reveals the micro-morphology of the Li-Ag@CF and Li-CF electrodes cycled at 1 mA cm^{-2} for 400 cycles. As shown, due to the homogeneous nucleation and plating/stripping of the Li, the Li-Ag@CF electrode achieved a uniform and flat surface, and no Li dendrite or dead Li can be observed. In contrast, a rougher surface with abundant gullies and mossy Li was observed on the unmodified Li-CF after 400 cycles. This indicates that the new modified composite electrodes in our strategy guarantee the homogeneous plating/stripping of Li during long cycling.

Figure 4c confirms the satisfactory rate performance of the Ag-modified composite electrodes with stable and mitigated voltage polarizations of 24 mV, 30 mV, 45 mV, 80 mV, and 125 mV at 0.5 mA cm^{-2}, 1 mA cm^{-2}, 2 mA cm^{-2}, 5 mA cm^{-2}, and 10 mA cm^{-2}, respectively. These are superior to those of the Li-CF electrodes, especially in the case of high current density. Nyquist tests were conducted to evaluate the charge transfer resistance of the Li-Ag@CF and Li-CF electrodes before and after 100 cycles (the equivalent circuit diagram is shown in Fig. S6). As can be seen in Fig. 4d, the interfacial resistance of the Li-Ag@CF and Li-CF electrodes before cycling are nearly equal, indicating that the Ag nanoparticles are tightly anchored on the surface of the CF skeleton and did not excessively increase the charge transfer resistance between the electrolyte and the electrode. After 100 cycles, the interfacial resistance of the Li-Ag@CF and Li-CF electrodes decreased to 4.1 Ω cm^{-2} and 5 Ω cm^{-2}, respectively. This is consistent with the performance of the over-potential change during cycling. A lower interfacial resistance after cycling implies the superior interface and excellent electrical conductivity of the Li-Ag@CF electrodes in cycling.

To emphasize the significance of the new design, full cells consisting of LFP and Li-Ag@CF or bare Li as the cathode and anode were assembled for investigation. As observed in Fig. 5a, a full cell assembled using Li-Ag@CF (LFP|Li-Ag@CF) displays an excellent cycling performance with the considerable capacity retention of 84.2% (118.2 mA h g^{-1}) after 800 cycles at 1 C (170 mA g^{-1}). In contrast, with a poor initial capacity, the LFP|Bare Li full cell displayed a rapidly decaying discharge capacity before 300 cycles. The excellent cycling performance of the LFP|Li-Ag@CF full cell was believed to originate from the enhanced Li-Ag@CF in which the CF, modified by Ag nanoparticles, plays a key role. In addition, the charge/discharge curves of the LFP|Li-Ag@CF full cell exhibited a much more stable capacity with reduced polarization voltage in the initial and subsequent cycles (Fig. S7). Superior cycling performance can also be observed

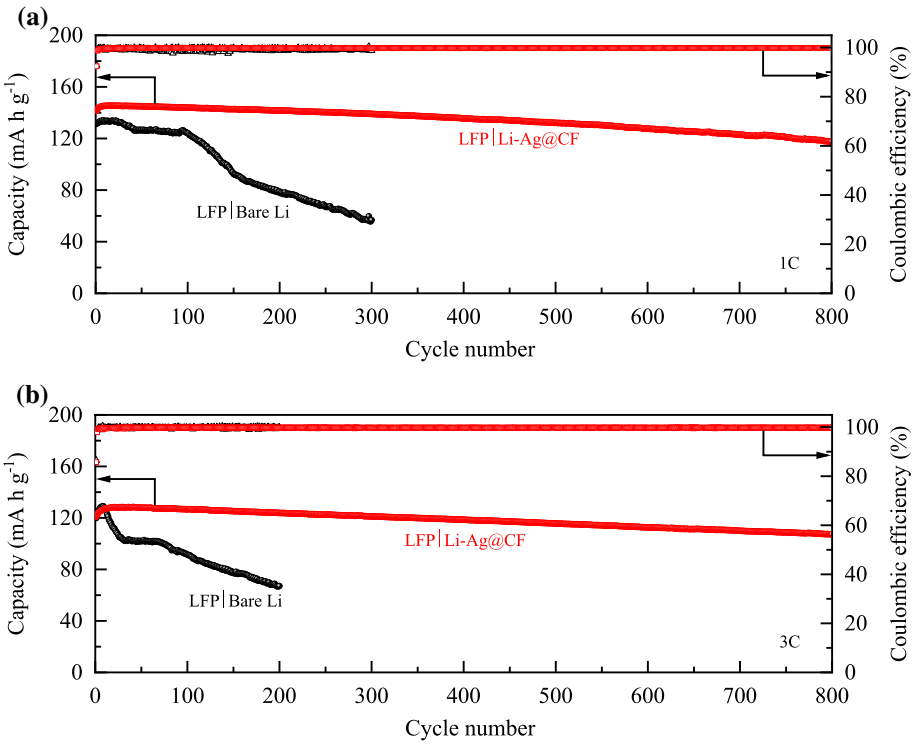

Fig. 5 Cycling performances of LFP|Li-Ag@CF and LFP|Bare Li full cells at 1 C (a) and 3 C (b)

in higher rate cases, with the LFP|Li-Ag@CF full cell delivering a much higher discharge capacity and capacity retention at 3 C (Fig. 5b).

Conclusions

A lithiophilic 3D Ag@CF collector has been designed and prepared via an ordinary displacement reaction under ultrasonic conditions. The porous structure of the Ag@CF collector alleviated the volume change of the Li-Ag@CF composite electrodes. Ag nanoparticles anchored on the surface of the CF skeleton significantly reduced the energy barrier of Li nucleation and deposition, resulting in a homogeneous plating/stripping of Li and inhibiting the growth of Li dendrites. With those advantages, symmetric cells assembled by the Li-Ag@CF electrodes delivered an ultra-long lifespan with a mitigated voltage hysteresis. In addition, using the Li-Ag@CF electrodes as anodes, full cells revealed enhanced cycling performances and capacity retention at 1 and 3 C. More importantly, the basic material is compatible with the current commercial anode current collector of LIBs, and the convenient preparation method guarantees that superior anode current collectors can be produced in a large scale.

Supplementary Information The online version contains supplementary material available at https://doi.org/10.1007/s11664-022-09598-4.

Acknowledgments This work was financially supported by National Key Research and Development Program of China (Grant No. 2017YFA0701001) and National Natural Science Foundation of China (Grant No. 52002052).

Conflict of interest The authors declare that they have no conflict of interest.

References

1. T. Ackermann, G. Andersson, and L. Soder, Distributed generation: a definition. *Electr. Power Syst. Res.* 57, 195 (2001).
2. M. Lukatskaya, B. Dunn, and Y. Gogotsi, Multidimensional materials and device architectures for future hybrid energy storage. *Nat. Commun.* 7, 12647 (2016).
3. G. Zubi, R. Dufo-Lopez, M. Carvalho, and G. Pasaoglu, The lithium-ion battery: state of the art and future perspectives. *Renew. Sustain. Energy Rev.* 89, 292 (2018).
4. G. Harper, R. Sommerville, E. Kendrick, L. Driscoll, P. Slater, R. Stolkin, A. Walton, P. Christensen, O. Heidrich, S. Lambert, A. Abbott, K.S. Ryder, L. Gaines, and P. Anderson, Recycling lithium-ion batteries from electric vehicles. *Nature* 575, 75 (2019).
5. X. Shan, Y. Zhong, L. Zhang, Y. Zhang, X. Xia, X. Wang, and J. Tu, A brief review on solid electrolyte interphase composition characterization technology for lithium metal batteries: challenges and perspectives. *J. Phys. Chem. C* 125, 19060 (2021).
6. T. Kim, W. Song, D.-Y. Son, L.K. Ono, and Y. Qi, Lithium-ion batteries: outlook on present, future, and hybridized technologies. *J. Mater. Chem. A* 7, 2942 (2019).
7. F. Wu, J. Maier, and Y. Yu, Guidelines and trends for next-generation rechargeable lithium and lithium-ion batteries. *Chem. Soc. Rev.* 49, 1569 (2020).

8. Y. Zhang, T. Zuo, J. Popovic, K. Lim, Y. Yin, J. Maier, and Y. Guo, Towards better Li metal anodes: challenges and strategies. *Mater. Today* 33, 56 (2020).
9. N. Li, Y. Yin, C. Yang, and Y. Guo, An artificial solid electrolyte interphase layer for stable lithium metal anodes. *Adv. Mater.* 28, 1853 (2016).
10. G. Zheng, S.W. Lee, Z. Liang, H.-W. Lee, K. Yan, H. Yao, H. Wang, W. Li, S. Chu, and Y. Cui, Interconnected hollow carbon nanospheres for stable lithium metal anodes. *Nat. Nanotechnol.* 9, 618 (2014).
11. Y. Wang and F. Qin, Effects of components in solvent-enhanced PVDF-HFP-based polymer electrolyte on its electrochemical performance. *J. Electron. Mater.* 50, 5049 (2021).
12. J. Pender, G. Jha, D. Youn, J. Ziegler, I. Andoni, E. Choi, A. Heller, B. Dunn, P. Weiss, R. Penner, and C. Mullins, Electrode degradation in lithium-ion batteries. *ACS Nano* 14, 1243 (2020).
13. Z. Huang, G. Zhou, W. Lv, Y. Deng, Y. Zhang, C. Zhang, F. Kang, and Q. Yang, Seeding lithium seeds towards uniform lithium deposition for stable lithium metal anodes. *Nano Energy* 61, 47 (2019).
14. P. Hundekar, S. Basu, J. Pan, S. Bartolucci, S. Narayanan, Z. Yang, and N. Koratkar, Exploiting self-heat in a lithium metal battery for dendrite healing. *Energy Storage Mater.* 20, 291 (2019).
15. K. Leung, F. Soto, K. Hankins, P. Balbuena, and K. Harrison, Stability of solid electrolyte interphase components on lithium metal and reactive anode material surfaces. *J. Phys. Chem. C* 120, 6302 (2016).
16. L. Yingying, M. Tikekar, R. Mohanty, K. Hendrickson, L. Ma, and L.A. Archer, Stable cycling of lithium metal batteries using high transference number electrolytes. *Adv. Energy Mater.* 5, 1402073 (2015). https://doi.org/10.1002/aenm.201402073.
17. A. Basile, A. Bhatt, and A. O'Mullane, Stabilizing lithium metal using ionic liquids for long-lived batteries. *Nat. Commun.* 7, 11794 (2016).
18. J. Chen, H. Yang, X. Zhang, J. Lei, H. Zhang, H. Yuan, J. Yang, Y. Nuli, and J. Wang, Highly reversible lithium-metal anode and lithium-sulfur batteries enabled by an intrinsic safe electrolyte. *ACS Appl. Mater. Interfaces.* 11, 33419 (2019).
19. L. Liang, X. Chen, W. Yuan, H. Chen, H. Liao, and Y. Zhang, Highly conductive, flexible, and nonflammable double-network poly(ionic liquid)-based ionogel electrolyte for flexible lithium-ion batteries. *ACS Appl. Mater. Interfaces.* 13, 25410 (2021).
20. B. Yuan, K. Wen, D. Chen, Y. Liu, Y. Dong, C. Feng, Y. Han, J. Han, Y. Zhang, C. Xia, A. Sun, and W. He, Composite separators for robust high rate lithium ion batteries. *Adv. Func. Mater.* 31, 2101420 (2021).
21. Y. Liu, D. Lin, P.Y. Yuen, K. Liu, J. Xie, R.H. Dauskardt, and Y. Cui, An artificial solid electrolyte interphase with high li-ion conductivity, mechanical strength, and flexibility for stable lithium metal anodes. *Adv. Mater.* 29, 1605531 (2017).
22. N. Li, Y. Shi, Y. Yin, X. Zeng, J. Li, C. Li, L. Wan, R. Wen, and Y. Guo, A flexible solid electrolyte interphase layer for long-life lithium metal anodes. *Angew. Chem. Int. Ed.* 57, 1505 (2018).
23. Y. Xu, Y. Zhou, T. Li, S. Jiang, X. Qian, Q. Yue, and Y. Kang, Multifunctional covalent organic frameworks for high capacity and dendrite-free lithium metal batteries. *Energy Storage Mater.* 25, 334 (2020).
24. T. Cai, Y. Lo, and J. Wu, Porous sulfide scaffolded solvent-free PEG-Ti hybrid polymer: all-solution-processed thin film composite polymer electrolytes directly on electrodes for lithium-ion batteries. *Mater. Today Energy* 13, 119 (2019).
25. L. Gao, J. Li, J. Ju, B. Cheng, W. Kang, and N. Deng, High-performance all-solid-state polymer electrolyte with fast conductivity pathway formed by hierarchical structure polyamide 6 nanofiber for lithium metal battery. *J. Energy Chem.* 54, 644 (2021).
26. D. Zhu, J. Hou, L. Zhang, Y. Gao, B. Dai, Y. Lian, H. Yan, and H. Zhang, Microbial porous carbon by low-alkali activation for flexible supercapacitors. *J. Electron. Mater.* 50, 6733 (2021).
27. L. Trung Hieu, N. Van Hoanh, N. Manh Tuong, N. Van Canh, V. Duy Nhan, P. Thanh Dong, and T. Dinh Trinh, Enhanced electrochemical performance of porous carbon derived from cornstalks for supercapacitor applications. *J. Electron. Mater.* 50, 6854 (2021).
28. S. Jin, Y. Jiang, H. Ji, and Y. Yu, Advanced 3D current collectors for lithium-based batteries. *Adv. Mater.* 30, 1802014 (2018).
29. Y. Yue and H. Liang, 3D current collectors for lithium-ion batteries: a topical review. *Small Methods* 2, 1800056 (2018).
30. Y. Zhan, P. Shi, X. Zhang, F. Ding, J. Huang, Z. Jin, R. Xiang, X. Liu, and Q. Zhang, The insights of lithium metal plating/stripping in porous hosts: progress and perspectives. *Energ. Technol.* 9, 2000700 (2021).
31. Q. Li, S. Zhu, and Y. Lu, 3D porous Cu current collector/li-metal composite anode for stable lithium-metal batteries. *Adv. Func. Mater.* 27, 1606422 (2017).
32. S. Chi, Y. Liu, W. Song, L. Fan, and Q. Zhang, Prestoring lithium into stable 3D nickel foam host as dendrite-free lithium metal anode. *Adv. Func. Mater.* 27, 1700348 (2017).
33. H. Umh, J. Park, J. Yeo, S. Jung, I. Nam, and J. Yi, Lithium metal anode on a copper dendritic superstructure. *Electrochem. Commun.* 99, 27 (2019).
34. M. Rahman, Y. Wong, G. Song, and C. Wen, A review on porous negative electrodes for high performance lithium-ion batteries. *J. Porous Mater.* 22, 1313 (2015).
35. D. Lin, Y. Liu, Z. Liang, H. Lee, J. Sun, H. Wang, K. Yan, J. Xie and Y. Cui, Layered reduced graphene oxide with nanoscale interlayer gaps as a stable host for lithium metal anodes. *Nat. Nanotechnol.* 11, 626 (2016).
36. T. Tang and Y. Hou, Multifunctionality of carbon-based frameworks in lithium sulfur batteries. *Electrochem. Energy Rev.* 1, 403 (2018).
37. C. Wang, Y. Li, F. Cao, Y. Zhang, X. Xia, and L. Zhang, Employing Ni-embedded porous graphitic carbon fibers for high-efficiency lithium-sulfur batteries. *ACS Appl. Mater. Interfaces* 14, 10457 (2022).
38. L. Huang, S. Shen, Y. Zhong, Y. Zhang, L. Zhang, X. Wang, X. Xia, X. Tong, J. Zhou, and J. Tu, Multifunctional hyphae carbon powering lithium sulfur batteries. *Adv. Mater.* 34, e2107415 (2021).
39. Y. Zheng, S. Zheng, H. Xue, and H. Pang, Metal-organic frameworks for lithium-sulfur batteries. *J. Mater. Chem. A* 7, 3469 (2019).
40. V. Shrivastav, S. Sundriyal, P. Goel, H. Kaur, S. Tuteja, K. Vikrant, K. Kim, U. Tiwari, and A. Deep, Metal-organic frameworks (MOFs) and their composites as electrodes for lithium battery applications: novel means for alternative energy storage. *Coord. Chem. Rev.* 393, 48 (2019).
41. L. Li, K. Zhong, Y. Dang, J. Li, M. Ruan, and Z. Fang, Chemical dealloying pore structure control of porous copper current collector for dendrite-free lithium anode. *J. Porous Mater.* 28, 1813 (2021).
42. K. Yan, Z. Lu, H. Lee, F. Xiong, P. Hsu, Y. Li, J. Zhao, S. Chu, and Y. Cui, Selective deposition and stable encapsulation of lithium through heterogeneous seeded growth. *Nat. Energy* 1, 16010 (2016).
43. C. Yang, Y. Yao, S. He, H. Xie, E. Hitz, and L. Hu, Ultrafine silver nanoparticles for seeded lithium deposition toward stable lithium metal anode. *Adv. Mater.* 29, 1702714 (2017).
44. L. Qin, H. Xu, D. Wang, J. Zhu, J. Chen, W. Zhang, P. Zhang, Y. Zhang, W. Tian, and Z. Sun, Fabrication of lithiophilic copper foam with interfacial modulation toward high-rate lithium metal anodes. *ACS Appl. Mater. Interfaces.* 10, 27764 (2018).

45. Z. Wondimkun, W. Tegegne, J. Shi-Kai, C. Huang, N. Sahalie, M. Weret, J. Hsu, P. Hsieh, Y. Huang, S. Wu, W. Su, and B. Hwang, Highly-LITHIOPHILIC Ag@PDA-GO film to suppress dendrite formation on cu substrate in anode-free lithium metal batteries. *Energy Storage Mater.* 35, 334 (2021).
46. Y. Zhao, S. Hao, L. Su, Z. Ma, and G. Shao, Hierarchical Cu fibers induced Li uniform nucleation for dendrite-free lithium metal anode. *Chem. Eng. J.* 392, 123691 (2020).
47. M. Zhu, K. Xu, D. Li, T. Xu, W. Sun, Y. Zhu, and Y. Qian, Guiding smooth Li plating and stripping by a spherical island model for lithium metal anodes. *ACS Appl. Mater. Interfaces.* 12, 38098 (2020).
48. H. Xia, Q. Xie, Y. Tian, Q. Chen, M. Wen, J. Zhang, Y. Wang, Y. Tang, and S. Zhang, High-efficient CoPt/activated functional carbon catalyst for Li-O2 batteries. *Nano Energy* 84, 105877 (2021).
49. D. Zhang, A. Dai, B. Fan, Y. Li, K. Shen, T. Xiao, G. Hou, H. Cao, X. Tao, and Y. Tang, Three-dimensional ordered macro/mesoporous Cu/Zn as a lithiophilic current collector for dendrite-free lithium metal anode. *ACS Appl. Mater. Interfaces.* 12, 31542 (2020).
50. J. Zhang, H. Chen, M. Wen, K. Shen, Q. Chen, G. Hou, and Y. Tang, Lithiophilic 3D copper-based magnetic current collector for lithium-free anode to realize deep lithium deposition. *Adv. Funct. Mater.* 32, 2110110 (2021).
51. J. Yu, Y. Dang, M. Bai, J. Peng, D. Zheng, J. Zhao, L. Li, and Z. Fang, Graphene-modified 3D copper foam current collector for dendrite-free lithium deposition. *Front. Chem.* 7, 748 (2019).
52. R. Zhang, X. Chen, X. Shen, X. Zhang, X. Chen, X. Cheng, C. Yan, C. Zhao, and Q. Zhang, Coralloid carbon fiber-based composite lithium anode for robust lithium metal batteries. *Joule* 2, 764 (2018).
53. Z. Huang, D. Kong, Y. Zhang, Y. Deng, G. Zhou, C. Zhang, F. Kang, W. Lv, and Q.-H. Yang, Vertical graphenes grown on a flexible graphite paper as an all-carbon current collector towards stable Li deposition. *Research* 2020, 1–11 (2020). https://doi.org/10.34133/2020/7163948.
54. Y. Cheng, X. Ke, Y. Chen, X. Huang, Z. Shi, and Z. Guo, Lithiophobic-lithiophilic composite architecture through co-deposition technology toward high-performance lithium metal batteries. *Nano Energy* 63, 103854 (2019).

Authors and Affiliations

Qiang Zhao[1,2] · Jiayan Li[1] · Xin Chen[1] · Yongqi Zhang[2,3]

[1] School of Materials and Energy, University of Electronic Science and Technology of China, Chengdu 611731, People's Republic of China

[2] Yangtze Delta Region Institute (Huzhou), University of Electronic Science and Technology of China, Huzhou 313001, People's Republic of China

[3] Institute of Fundamental and Frontier Sciences, University of Electronic Science and Technology of China, Chengdu 610054, Sichuan, People's Republic of China